Extending the Higgs sector: an extra singlet.

S.I. Godunov,[1,2,*] A.N. Rozanov,[3] M.I. Vysotsky,[1,4,5,†] and E.V. Zhemchugov[1,5,‡]

[1] *Institute for Theoretical and Experimental Physics, Moscow, 117218, Russia*

[2] *Novosibirsk State University, Novosibirsk, 630090, Russia*

[3] *The Center for Particle Physics of Marseilles, Marseille, F-13288, France*

[4] *Moscow Institute of Physics and Technology,*

141700, Dolgoprudny, Moscow Region, Russia

[5] *Moscow Engineering Physics Institute, 115409, Moscow, Russia*

Abstract

An extension of the Standard Model with an additional Higgs singlet is analyzed. Bounds on singlet admixture in 125 GeV h boson from electroweak radiative corrections and data on h production and decays are obtained. Possibility of double h production enhancement at 14 TeV LHC due to heavy higgs contribution is considered.

* sgodunov@itep.ru

† vysotsky@itep.ru

‡ zhemchugov@itep.ru

I. INTRODUCTION

After the discovery of the Higgs (BEH) boson [1, 2], all fundamental particles of the Standard Model (SM) are finally found, and now even passionate adepts of the SM should look for physics beyond it. The pattern of particles we have is rather asymmetric: there are twelve vector bosons, many leptons and quarks with spin 1/2 and only one scalar particle h with mass 125 GeV. Of course, there is only one particle with spin 2 as well, a graviton. However, unlike the spin 2 case, there are no fundamental principle according to which there should exist only one fundamental scalar particle. That is why it is quite probable that there are other still undiscovered fundamental scalar particles in Nature. The purpose of the present paper is to consider the simplest extension of the SM by adding one real scalar field to it. Such an extension of the SM attracts considerable attention: relevant references can be found in recent papers [3–6]. Extra singlet can provide first order electroweak phase transition needed for electroweak baryogenesis. It can act as a particle which connects SM particles to Dark Matter. Not going into these (very interesting) applications, we will study the degree of enhancement of double higgs production at LHC due to an extra singlet. To do this we should analyze bounds on the mass of the additional scalar particle and its mixing with isodoublet state.

An enhancement of hh production occurs due to the mixing of the SM isodoublet with additional scalar field which is proportional to the vacuum expectation value (vev) of this field. Thus isosinglet is singled out: its vev does not violate custodial symmetry and can be large. For higher representations special care is needed; see paper [7] where an introduction of isotriplet(s) in the SM is discussed.

The paper is organized as follows: in Section II we describe the model and find the physical states. In Section III we get bounds on the model parameters of the scalar sector from the experimental data on h production and decays and from precision measurements of Z- and W-boson parameters and t-quark and h masses. In Section IV we discuss double h production at LHC Run 2. In Appendix A qualititative description of single and double higgs production at LHC is presented.

II. THE MODEL

Adding to the SM a real field X, we take the scalar fields potential in the following form:

$$V(\Phi, X) = -\frac{m_\Phi^2}{2}\Phi^\dagger\Phi + \frac{m_X^2}{2}X^2 + \frac{\lambda}{2}(\Phi^\dagger\Phi)^2 + \mu\Phi^\dagger\Phi X, \tag{1}$$

where Φ is an isodoublet.[1] Terms proportional to X^3, X^4 and $\Phi^\dagger\Phi X^2$ are omitted despite that they are allowed by the demand of renormalizability: we always may assume that they are multiplied by small coupling constants. Two combinations of the parameters entering (1) are known experimentally: it is the mass of one of the two scalar states, h, which equals 125 GeV and the isodoublet expectation value $v_\Phi = 246$ GeV. The two remaining combinations are determined by the mass of the second scalar, H (we take $m_H > m_h$, though this is not obligatory), and the angle α which describes singlet-doublet admixture:

$$\begin{cases} h = \phi\cos\alpha + \chi\sin\alpha, \\ H = -\phi\sin\alpha + \chi\cos\alpha, \end{cases} \qquad \begin{cases} \phi = h\cos\alpha - H\sin\alpha, \\ \chi = h\sin\alpha + H\cos\alpha. \end{cases} \tag{2}$$

Substituting in (1)

$$\Phi = \begin{pmatrix} \phi^+ \\ \frac{1}{\sqrt{2}}(v_\Phi + \phi + i\eta) \end{pmatrix}, \qquad X = v_X + \chi, \tag{3}$$

at the minimum of the potential we get:

$$\begin{cases} \lambda v_\Phi^2 + 2\mu v_X = m_\Phi^2, \\ 2m_X^2 v_X + \mu v_\Phi^2 = 0, \end{cases} \tag{4}$$

so μ is negative. For the mass matrix using (4) we get:

$$M = \begin{pmatrix} V_{\phi\phi} & V_{\phi\chi} \\ V_{\phi\chi} & V_{\chi\chi} \end{pmatrix} = \begin{pmatrix} \lambda v_\Phi^2 & \mu v_\Phi \\ \mu v_\Phi & m_X^2 \end{pmatrix}, \tag{5}$$

where $V_{\phi\chi} \equiv \frac{\partial^2 V}{\partial\phi\partial\chi}, \ldots$ Eigenvalues of (5) determine masses of scalar particles:

$$m_{h,H}^2 = \frac{1}{2}\lambda v_\Phi^2 + \frac{1}{2}m_X^2 \mp \sqrt{\left(\frac{1}{2}\lambda v_\Phi^2 - \frac{1}{2}m_X^2\right)^2 + \mu^2 v_\Phi^2}, \tag{6}$$

[1] We are grateful to J. M. Frère who brought to our attention that similar model was considered long ago in [8].

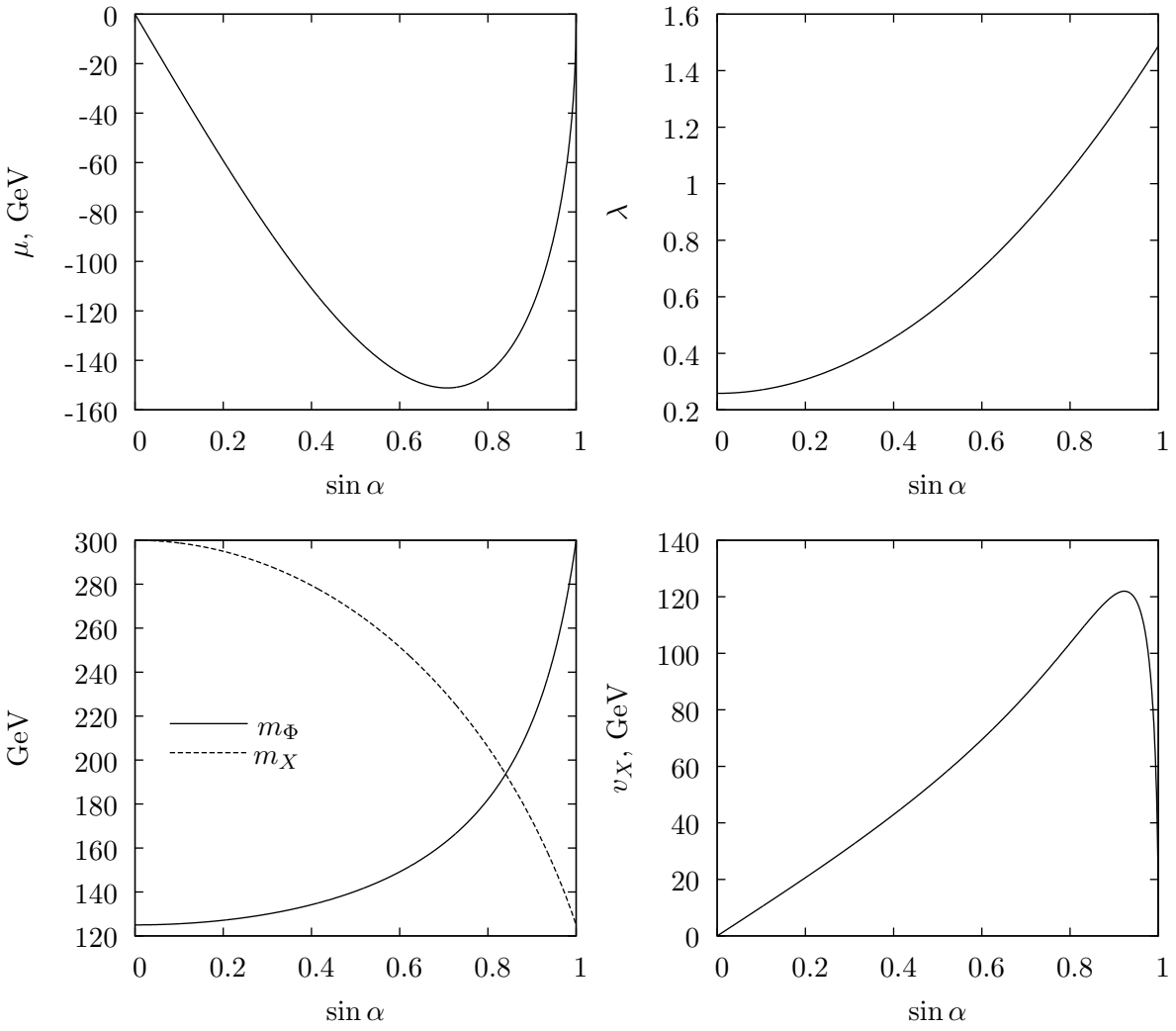

FIG. 1: Dependencies of the model parameters on the mixing angle for $m_H = 300$ GeV.

where "−" corresponds to m_h and "+"—to m_H. Eigenfunctions are determined by the mixing angle α:

$$\sin 2\alpha = \frac{-2\mu v_\Phi}{m_H^2 - m_h^2}, \quad \tan\alpha = \frac{m_h^2 - \lambda v_\Phi^2}{\mu v_\Phi}. \tag{7}$$

Equations (7) determine μ and λ for the given mixing angle α, while equations (6) determine m_X for given α as well. Finally, equations (4) determine the values of m_Φ and v_X. Fig. 1 demonstrates the dependencies just described for $m_H = 300$ GeV.

III. BOUNDS FROM h PRODUCTION AT LHC AND ELECTROWEAK PRECISION OBSERVABLES

ATLAS and CMS collaborations had detected h production and decays in the reactions

$$pp \to h \to f_i, \tag{8}$$

where $f_i, i = 1, 2, \ldots, 5$ designate the so-called "Big five" final state channels: WW^*, ZZ^*, $\gamma\gamma$, $\tau\bar{\tau}$, $b\bar{b}$. Cross sections of reactions (8) are equal to the higgs production cross section times branching ratio of the corresponding decay channel. Quantities μ_i are introduced according to the following definition:

$$\mu_i \equiv \frac{\sigma_{pp\to h} \cdot \Gamma_{h\to f_i}/\Gamma_h}{(\sigma_{pp\to h} \cdot \Gamma_{h\to f_i}/\Gamma_h)_{\rm SM}}. \tag{9}$$

According to ATLAS and CMS results, all μ_i are compatible with one within experimental and theoretical accuracy. It means that no New Physics are up to now observed in h production and decays.

In the model with an extra isosinglet, production and decay probabilities of h equal that in the SM multiplied by a factor $\cos^2\alpha$, that is why we have:

$$\mu_i = \cos^2\alpha, \tag{10}$$

and existing bounds on μ_i are translated into bounds on the mixing angle α. Taking into account all measured production and decay channels, for the average values experimentalists obtain [9, 10]:

$$\text{ATLAS:} \qquad \mu = 1.30^{+0.18}_{-0.17}, \tag{11}$$

$$\text{CMS:} \qquad \mu = 1.00^{+0.14}_{-0.13}\left[\pm 0.09(\text{stat.})^{+0.08}_{-0.07}(\text{theor.}) \pm 0.07(\text{syst.})\right] \tag{12}$$

Let us stress that the theoretical uncertainty in the calculation of $pp \to h$ production cross section at LHC does not allow to reduce substantially the uncertainty in the value of μ. Bounds from electroweak precision observables (EWPO) are not affected by this particular uncertainty.

We fit experimental data with the help of LEPTOP program [11] using $m_h = 125.14$ GeV. The result of the SM fit which accounts the h mass measurement is shown in Table I. Quality of the fit is characterised by the χ^2 value

$$\chi^2/n_{\rm d.o.f.} = 19.6/13. \tag{13}$$

TABLE I: EWPO fit of the Standard Model

Observable	Experimental value	Standard Model	Pull
Γ_Z, GeV	2.4952(23)	2.4966(14)	−0.5895
σ_h, nb	41.541(37)	41.475(14)	1.7746
R_l	20.771(25)	20.744(18)	1.0831
$A^l_{\rm FB}$	0.0171(10)	0.0165(2)	0.6572
A_τ	0.1439(43)	0.1484(7)	−1.0452
R_b	0.2163(7)	0.2158(0)	0.7699
R_c	0.1721(30)	0.1722(0)	−0.0277
$A^b_{\rm FB}$	0.0992(16)	0.1040(5)	−3.0303
$A^c_{\rm FB}$	0.0707(35)	0.0744(4)	−1.0565
s^2_l $(Q_{\rm FB})$	0.2324(12)	0.2313(1)	0.8771
$A_{\rm LR}$	0.1514(22)	0.1484(7)	1.3822
A_b	0.923(20)	0.9349(1)	−0.5941
A_c	0.670(27)	0.6685(3)	0.0567
M_W, GeV	80.3846(146)	80.3725(67)	0.8322
m_t, GeV	173.24(95)	174.32(89)	−1.1370
$1/\bar{\alpha}$	128.954(48)	129.023(37)	−1.4378

Higgs boson contributions to electroweak observables at one loop are described in LEPTOP by functions $H_i(h) = H_i(m_h^2/m_Z^2)$. In the case of an extra singlet the following substitution should be performed:

$$H_i(h) \to \cos^2\alpha\, H_i(h) + \sin^2\alpha\, H_i(H),\ H = m_H^2/m_Z^2. \tag{14}$$

The same substitution should be made for the functions $\delta_4 V_i(t,h)$, $t = m_t^2/m_Z^2$, which describe two loops radiative corrections enhanced as m_t^4. In two loops quadratic dependence on higgs mass appears which is described by functions $\delta_5 V_i$. Calculations of these corrections in the case of an extra singlet higgs is not easy. An approximate upper bound has been estimated by assuming that

$$\delta_5 V_i(H) < \delta_5 V_i((1000\ {\rm GeV})^2/m_Z^2) \approx 100\ \delta_5 V_i(h) \text{ for } m_H < 1000\ {\rm GeV}. \tag{15}$$

Comparison of two calculations, one with $\delta_5 V_i(h) = \cos^2\alpha\ \delta_5 V_i(h)$, and the other with

$$\delta_5 V_i(h) = \cos^2\alpha\ \delta_5 V_i(h) + 100 \cdot \sin^2\alpha\ \delta_5 V_i(h), \tag{16}$$

showed that the correction to the values of $\sin\alpha$ in Fig. 2 is less than 10^{-3}.

Bounds from EWPO on the singlet model parameters are presented in Fig. 2a. χ^2 minimum is reached at $\sin\alpha = 0$, $m_H = 150$ GeV, which is the minimum value allowed for m_H in the fit. Experimental data are avoiding heavy higgs. The value of χ^2 at the minimum coincides with the SM result (13). Lines of constant χ^2 correpospond to $\Delta\chi^2 = 1, 4, 9, \ldots$. Probabilities that $(\sin\alpha, m_H)$ values are below these lines are 39%, 86%, 98.9%, ...[2]

Bounds accounting for both EWPO and direct h production data (11), (12) are shown in Fig. 2b. We see that for heavy H bounds from EWPO dominate, while for light H measurement of μ is more important.

IV. h, H AND hh PRODUCTION AT LHC

The main purpose of this section is to find what enhancement of double higgs production cross section is possible with enlarged higgs sector. Let us remind that in the SM double h production cross section is very small. According to the recent result [16], at $\sqrt{s} = 14$ TeV $\sigma^{\rm NNLO}(pp \to hh) = 40$ fb with a $10 \div 15\%$ accuracy. We will demonstrate that enlarged higgs sector allows to strongly enhance double h production.

The cross section of H production at LHC equals that for the SM higgs production (for $(m_h)_{\rm SM} = m_H$) multiplied by $\sin^2\alpha$. Cross section of the SM higgs production at NNLO we take from Table 3 of [15]. In order to obtain cross section of resonant hh production in H decays we should multiply cross section of H production by ${\rm Br}(H \to hh)$.

Let us consider H decays. Decays to hh, W^+W^-, ZZ and $t\bar{t}$ dominate. For the Hhh coupling we obtain:

$$\begin{aligned}
\Delta\mathcal{L}_{Hhh} &= \left[\frac{3}{2}\lambda v_\Phi \cos^2\alpha \sin\alpha - \frac{\mu}{2}\cos\alpha(1 - 3\sin^2\alpha)\right] Hh^2 \\
&= \frac{2m_h^2 + m_H^2}{2v_\Phi}\sin\alpha\cos^2\alpha\ Hh^2 \\
&\equiv g_{Hhh} Hh^2,
\end{aligned} \tag{17}$$

[2] Let us note that if a subset of experimental data from Table I is fitted, then allowed domains of the $(\sin\alpha, m_H)$ values will be larger than those presented in Fig. 2a. Here we disagree with the statement made in [4] that the fit of only one observable (m_W) allows to set the strongest constraint on $(\sin\alpha, m_H)$.

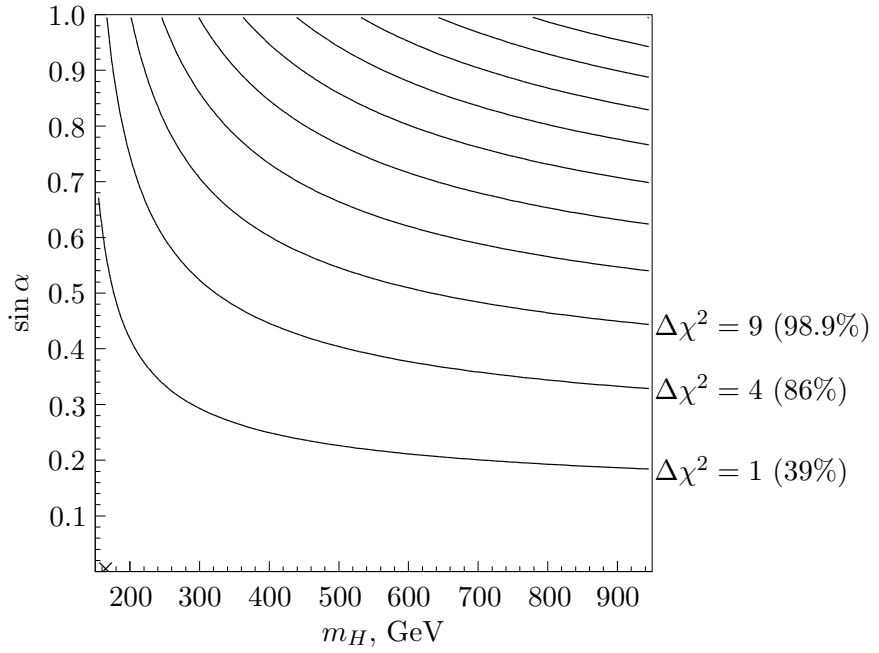

(a) Bounds from electroweak precision observables.

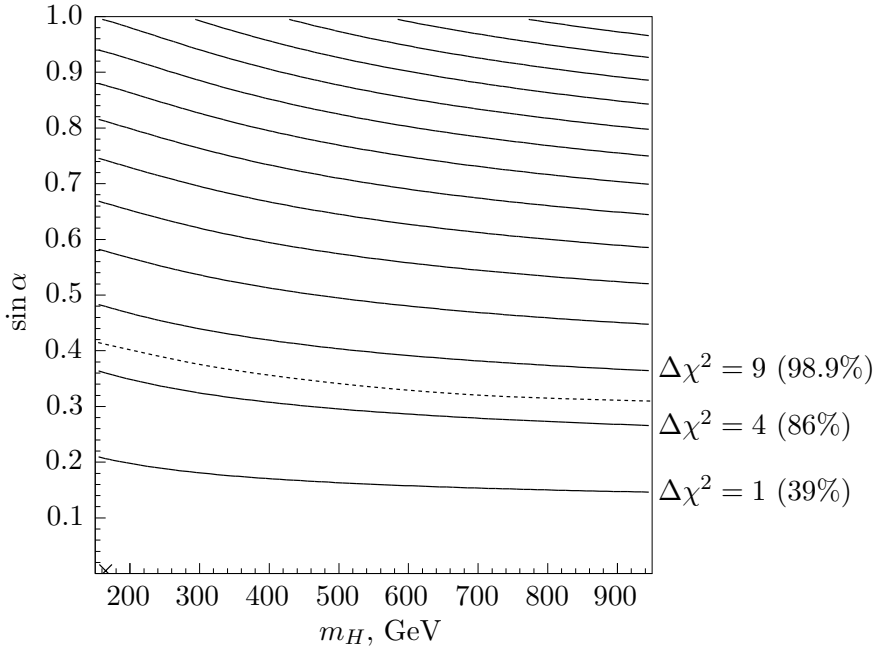

(b) Bounds from both electroweak precision observables and signal strength measurements (11), (12). The dashed line corresponds to $\Delta\chi^2 = 5.99$; the probability that numerical values of $(m_H, \sin\alpha)$ are below it equals 95% (compare with Ref. [6], eq. (23)).

FIG. 2: Bounds on the singlet model parameters.

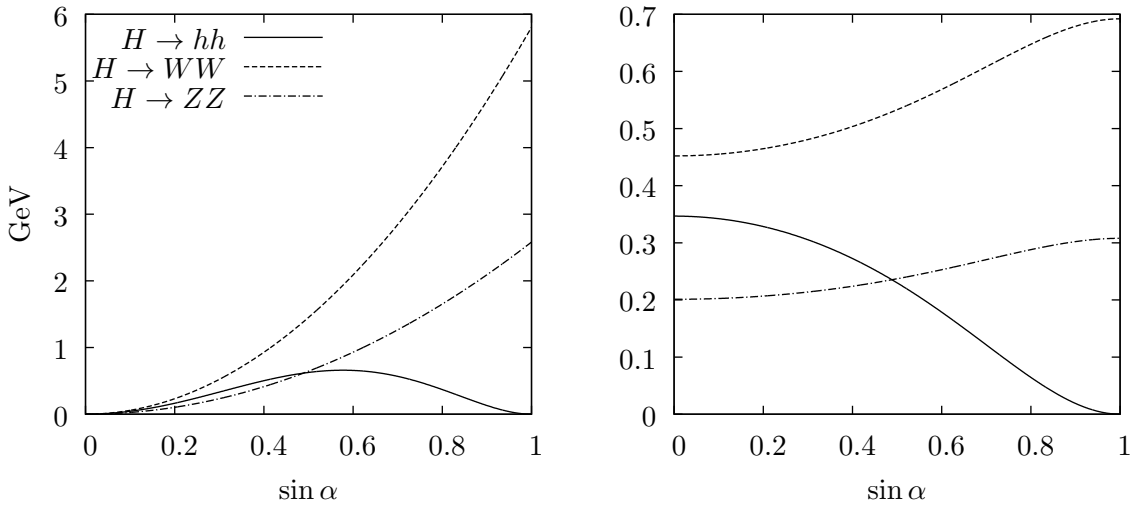

(a) Decay widths.

(b) Branching ratios.

FIG. 3: Decay widths and branching ratios of the heavy higgs boson for $m_H = 300$ GeV.

thus

$$\Gamma_{H\to hh} = \frac{g_{Hhh}^2}{8\pi m_H}\sqrt{1-\left(\frac{2m_h}{m_H}\right)^2}. \tag{18}$$

Decays to W^+W^-, ZZ, $t\bar{t}$ occur through isodoublet admixture in H:

$$\begin{aligned}\Delta\mathcal{L} &= \frac{2m_W^2}{v_\Phi}\sin\alpha\ HW^+W^- + \frac{m_Z^2}{v_\Phi}\sin\alpha\ HZ^2 + \frac{m_t}{v_\Phi}\sin\alpha\ Ht\bar{t} \\ &\equiv g_{HWW}HW^+W^- + \frac{1}{2}g_{HZZ}HZ^2 + g_{Ht\bar{t}}Ht\bar{t},\end{aligned} \tag{19}$$

thus

$$\Gamma_{H\to W^+W^-} = \frac{g_{HWW}^2 m_H^3}{64\pi m_W^4}\left[1-4\frac{m_W^2}{m_H^2}+12\frac{m_W^4}{m_H^4}\right]\sqrt{1-\left(\frac{2m_W}{m_H}\right)^2}, \tag{20}$$

$$\Gamma_{H\to ZZ} = \frac{g_{HZZ}^2 m_H^3}{128\pi m_Z^4}\left[1-4\frac{m_Z^2}{m_H^2}+12\frac{m_Z^4}{m_H^4}\right]\sqrt{1-\left(\frac{2m_Z}{m_H}\right)^2}, \tag{21}$$

$$\Gamma_{H\to t\bar{t}} = \frac{3g_{Ht\bar{t}}^2 m_H}{8\pi}\left[1-\left(\frac{2m_t}{m_H}\right)^2\right]^{\frac{3}{2}}. \tag{22}$$

The dependence of the widths and branching ratios of H decays on mixing angle α for $m_H = 300$ GeV are shown in Figure 3.

For the cross section of the reaction $pp \to H \to hh$ we have:

$$\sigma(pp\to H\to hh) = \sigma(pp\to h)_{\rm SM}\cdot\sin^2\alpha\cdot{\rm Br}(H\to hh), \tag{23}$$

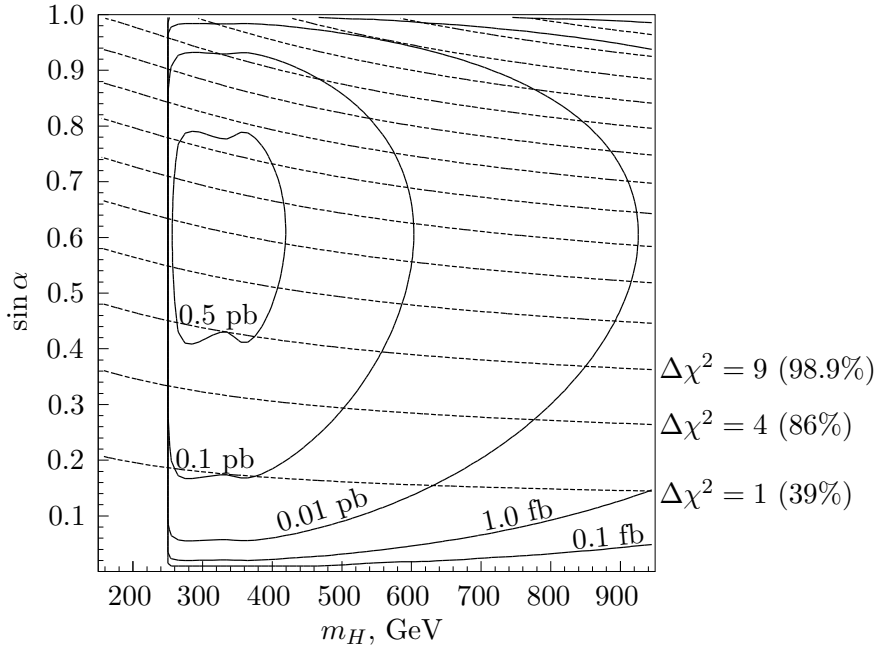

FIG. 4: Contour plot of $\sigma(pp \to H \to hh)$ for $\sqrt{s} = 14$ TeV.
In this figure we neglect small effects of $H \to hh^*$.

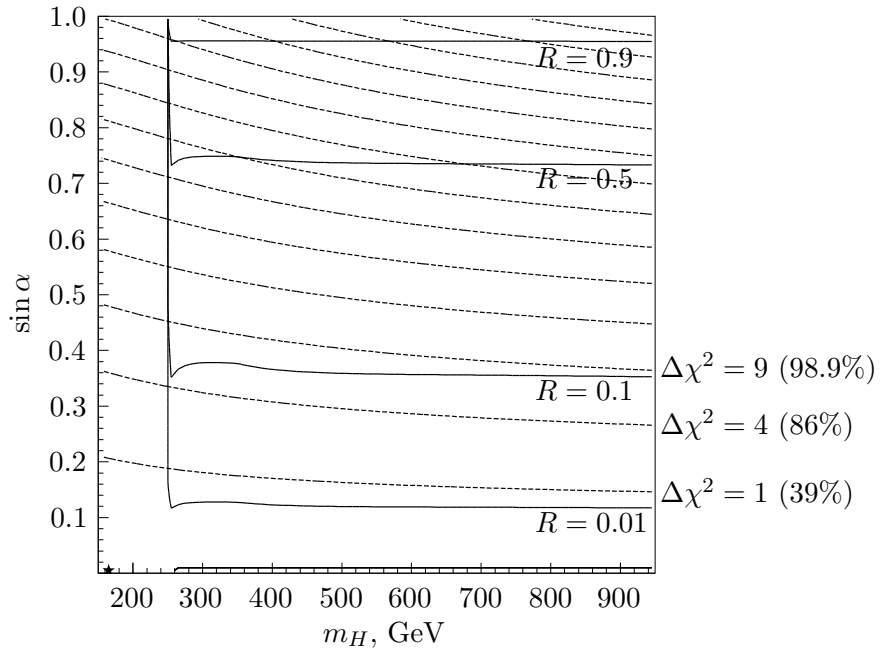

FIG. 5: Contour plot of $R \equiv \frac{\sigma(pp\to H)\mathrm{Br}(H\to ZZ)}{(\sigma(pp\to h)\mathrm{Br}(h\to ZZ))_{\mathrm{SM}}}$.
In the calculation of R we assume $m_H > 2m_h$.

the lines of constant cross section are shown in Fig. 4 (compare to Fig. 4 from [6]). $H \to ZZ$ decay can be used in order to find H; its cross section divided by that for the SM higgs boson with $(m_h)_{\rm SM} = m_H$ is

$$R \equiv \frac{\sigma(pp \to H) \cdot {\rm Br}(H \to ZZ)}{(\sigma(pp \to h) \cdot {\rm Br}(h \to ZZ))_{\rm SM}} = \frac{\sin^4 \alpha}{\sin^2 \alpha + \frac{\Gamma(H \to hh)}{\Gamma_{\rm SM}}}. \qquad (24)$$

Contour plot of R is presented in Fig. 5. Let us note that R does not depend on $\sqrt{s}$.

V. CONCLUSIONS

In the models with extended higgs sector strong resonant enhancement of double higgs production is possible which makes the search of $pp \to hh$ reaction at Run 2 LHC especially interesting. According to Fig. 4 cross section of $pp \to H \to hh$ reaction can be as large as 0.5 pb, ten times larger than the SM value.

The search for H boson can also go in the same way as it was for the heavy SM boson h. Probability of H observation diminishes compared to that of h because of a) suppression of H production cross section by the factor $\sin^2 \alpha \leq 0.2$; b) suppression of ${\rm Br}(H \to ZZ)$ because of additional $H \to hh$ decay mode. Taking these two factors into account, we get about factor 10 suppression of $pp \to H \to ZZ$ process probability compared to that for the SM higgs boson (see Fig. 5).

Results for the search of higgs-like boson in ZZ decay mode can be found in [20], Figure 5. Comparing it with our Fig. 5, we observe that experimental data start to be sensitive to the singlet model expectation for maximally allowed values of the mixing angle α.

After the first version of this paper was published in arXiv, we got a number of emails providing us with references to related research [21].

S. G., M. V. and E. Zh. are partially supported under the grants RFBR No. 14-02-00995 and NSh-3830.2014.2. S G. and E. Zh. are also supported by MK-4234.2015.2. In addition, S. G is supported by Dynasty Foundation and by the Russian Federation Government under grant No. 11.G34.31.0047.

Appendix A: Higgs production in effective Lagrangian approach

Simple analythical formulas which qualititavely describe single and double higgs production in the SM are presented in this section. Let us start with single higgs production in gluon fusion. In the limit $m_h \ll 2m_t$, the amplitude of $gg \to h$ transition is determined by the top quark contribution into the QCD Gell-Mann-Low function:

$$\Delta\mathcal{L} = \frac{\alpha_s}{12\pi} \ln\left(1 + \frac{h}{v_\Phi}\right) G^2_{\mu\nu}; \quad M = \frac{\alpha_s}{6\pi v_\Phi} G^1_{\mu\nu} G^2_{\mu\nu} h, \tag{A1}$$

leading to the well-known result for the production cross section:

$$\sigma_{gg\to h} = \frac{\alpha_s^2 \tau_0}{576\pi v_\Phi^2} \delta(\tau - \tau_0). \tag{A2}$$

Here $\tau = \hat{s}/s$ and $\tau_0 = m_h^2/s$; $s \equiv (p_1 + p_2)^2$ is the invariant mass of colliding protons, $\hat{s} = x_1 x_2 s \equiv \tau s$ is the invariant mass of colliding gluons. Integrating over gluons distribution in a proton, we get:

$$\sigma_{pp\to h} = \int\limits_{\tau_0}^{1} dx_1 \int\limits_{\tau_0/x_1}^{1} dx_2 \; g(x_1) g(x_2) \sigma_{gg\to h}. \tag{A3}$$

Changing the variables from x_1, x_2 to τ, y according to the following definitions: $x_1 = \sqrt{\tau}\mathrm{e}^{y}$, $x_2 = \sqrt{\tau}\mathrm{e}^{-y}$, and substituting (A2) into (A3), we obtain:

$$\sigma_{pp\to h} = \frac{\alpha_s^2 m_h^2}{576\pi v_\Phi^2} \frac{1}{s} \int\limits_{\ln\sqrt{\tau_0}}^{-\ln\sqrt{\tau_0}} g(\sqrt{\tau_0}\mathrm{e}^{y}) g(\sqrt{\tau_0}\mathrm{e}^{-y}) dy \equiv \frac{\alpha_s^2 m_h^2}{576\pi v_\Phi^2} \frac{dL}{d\hat{s}}, \tag{A4}$$

where the so-called gluon-gluon luminosity is given by the integral over gluon distributions:

$$\left.\frac{dL}{d\hat{s}}\right|_{\hat{s}=m_h^2} = \frac{1}{s} \int\limits_{\ln\sqrt{\tau_0}}^{-\ln\sqrt{\tau_0}} g(\sqrt{\tau_0}\mathrm{e}^{y}) g(\sqrt{\tau_0}\mathrm{e}^{-y}) dy. \tag{A5}$$

A number of PDFs parametrizations exist in the literature; their results for (A5) at $\sqrt{s} = 7$, 8, 14 and 100 TeV and $m_h^2 = (125\ \mathrm{GeV})^2$ coincide within several percents. Finite value of $m_t = 172$ GeV should be taken into account by multiplication of the leading order result for the amplitude M (A1) by a factor

$$F = \frac{3}{2}\beta[(1-\beta)x^2 + 1], \tag{A6}$$

where $\beta = \left(\dfrac{2m_t}{m_h}\right)^2$, and $x = \arctan\dfrac{1}{\sqrt{\beta - 1}}$ for $\beta > 1$, $x = \dfrac{1}{2}\left(\pi + i \ln\dfrac{1+\sqrt{1-\beta}}{1-\sqrt{1-\beta}}\right)$ for $\beta < 1$ [14] (note that $\lim\limits_{m_t\to\infty} F = 1$). This adjustment leads to 6% enlargement of $\sigma_{gg\to h}$

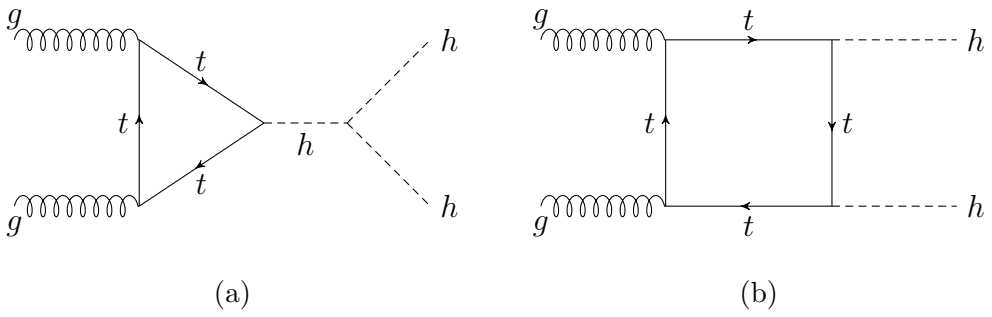

FIG. 6: Leading-order diagrams for the double higgs production at LHC.

compared to $m_t \to \infty$ value; however taking into account b and c quark contributions results in 6% overall reduction.

Applying all these factors and using PDFs from [12], we obtain numbers presented in Table II. To calculate $\sigma^{\rm NNLO}$ from $\sigma^{\rm LO}$ we use K-factor from [13]: $K \approx 2.5$ for $\sqrt{s} = 7$ and 8 TeV, and $K \approx 2$ for $\sqrt{s} = 14$ TeV. For $\sqrt{s} = 100$ TeV $K \approx 1.5$ (A. Djouadi, private communication). Let us stress that according to [13], accuracy of the calculated value of $\sigma^{\rm NNLO}_{pp\to h}$ is at the level of $\pm(10 \div 17)\%$ which makes hopes of reducing uncertainty in μ_i (and μ) below 10% elusive. In the case of an extra singlet, h and H production cross sections equal the SM one multiplied by $\cos^2\alpha$ and $\sin^2\alpha$ respectively.

Let us turn now to double h production at pp collision in the SM. At the leading order it is described by the two diagrams shown in Fig. 6. According to equations (4) and (11) and Table 1 from [17], the cross section of the double production of the 125 GeV h at 14 TeV LHC in the leading order equals:

$$\sigma^{\rm LO}(pp \to hh) = 144.6 \cdot \left(0.169^2 + 0.457^2 - 1.79 \cdot 0.457 \cdot 0.169\right)\ \text{fb} = 14\ \text{fb}, \qquad \text{(A7)}$$

where the first term in parentheses originates from the square of the triangle diagram, the second—from the square of the box diagram, while the last one is their interference, which diminishes the cross section.

In order to understand result (A7) let us proceed in the following way. In the limit $\hat{s} \ll 4m_t^2$ the triangle $gg \to h$ and box $gg \to hh$ amplitudes can be directly extracted from lagrangian (A1), expanding it over h/v_Φ:

$$\Delta\mathcal{L} = \frac{\alpha_s}{12\pi} \ln\left(1 + \frac{h}{v_\Phi}\right) G^2_{\mu\nu} = \frac{\alpha_s}{12\pi}\left(\frac{h}{v_\Phi} - \frac{1}{2}\frac{h^2}{v_\Phi^2}\right) G^2_{\mu\nu}, \qquad \text{(A8)}$$

where the first term corresponds to the diagram shown in Fig. 6a, while the second term

TABLE II: Data relevant for the SM higgs boson production at LHC. The difference between the numbers in Tables IIc and IId is due to poor accuracy of K-factors presented in [13].

(a) $\frac{dL}{d\hat{s}}$, 10^{-3} GeV^{-2}.

m_H \ $\sqrt{s}$	7 TeV	8 TeV	14 TeV	100 TeV
125 GeV	6.41	8.30	22.9	451
300 GeV	0.147	0.205	0.737	25.1

(b) $\sigma^{\rm LO}(pp \to h)$, pb.

m_H \ $\sqrt{s}$	7 TeV	8 TeV	14 TeV	100 TeV
125 GeV	5.52	7.16	19.8	389
300 GeV	0.936	1.31	4.69	160

(c) $\sigma^{\rm NNLO}(pp \to h)$, pb.

m_H \ $\sqrt{s}$	7 TeV	8 TeV	14 TeV	100 TeV
125 GeV	13.8	17.9	39.6	583
300 GeV	2.34	3.27	9.37	239

(d) $\sigma^{\rm NNLO}(pp \to h)$, pb, from Tables 1, 3 of [15].

m_H \ $\sqrt{s}$	7 TeV	8 TeV	14 TeV	100 TeV
125 GeV	15.31	N/A	49.97	N/A
300 GeV	2.42	N/A	11.07	N/A

describes the diagram shown in Fig. 6b. Triple higgs coupling is given by the following term in the SM lagrangian:

$$\Delta\mathcal{L} = \frac{m_h^2}{2v_\Phi} h^3, \tag{A9}$$

which leads to $\lambda_{hhh} = 3m_h^3/v_\Phi$. Hence, for the sum of the triangle and the box diagrams at

$\hat{s} \ll 4m_t^2$ we get

$$M = \frac{\alpha_s}{6\pi v_\Phi}\left[\frac{1}{\hat{s}-m_h^2}\cdot 3\frac{m_h^2}{v_\Phi} - \frac{1}{v_\Phi}\right] G^1_{\mu\nu}G^2_{\mu\nu}, \tag{A10}$$

which equals zero at threshold when $\hat{s} = (2m_h)^2$ [18, 19]. For the cross section we get

$$\hat{\sigma}_{gg\to hh}|_{\hat{s}\ll 4m_t^2} = \frac{\alpha_s^2 G_F^2 \hat{s}}{576(2\pi)^3}\left[1-\frac{3m_h^2}{\hat{s}-m_h^2}\right]^2\sqrt{1-\frac{(2m_h)^2}{\hat{s}}} \tag{A11}$$

(see Eq. 13 from [18]).

In the high-energy limit $\hat{s} \gg 4m_t^2$ box diagram dominates and the cross section behaves as:

$$\hat{\sigma}_{gg\to hh}|_{\hat{s}\gg 4m_t^2} = A^2\frac{\alpha_s^2}{16\pi^3\hat{s}}\left(\frac{m_t}{v_\Phi}\right)^4\sqrt{1-\frac{(2m_h)^2}{\hat{s}}}. \tag{A12}$$

Normalization constant A is determined by the condition that at $\hat{s} = 4m_t^2$ expressions (A11) and (A12) are equal:

$$A = \frac{1}{6}\left[1-\frac{3m_h^2}{4m_t^2-m_h^2}\right]. \tag{A13}$$

Finally, for the cross section of double h production in the SM we obtain the following approximate expression:

$$\sigma_{pp\to hh} = \int\limits_{(2m_h)^2}^{s} d\hat{s}\ \hat{\sigma}_{gg\to hh}(\hat{s})\frac{dL}{d\hat{s}}, \tag{A14}$$

$$\frac{dL}{d\hat{s}} = \frac{1}{s}\int\limits_{\ln\sqrt{\tau}}^{-\ln\sqrt{\tau}} g(\sqrt{\tau}\mathrm{e}^{y})g(\sqrt{\tau}\mathrm{e}^{-y})dy, \tag{A15}$$

where Equations (A11)–(A13) should be substituted in (A14) and $\tau \equiv \hat{s}/s$, $\hat{s}$ being the hh invariant mass. The differential cross section is shown in Fig. 7, while for the total cross section for hh production in the SM we get $\sigma(pp \to hh) = 4$ fb at $\sqrt{s} = 14$ TeV, 3.5 times smaller than the explicit leading order result (A7).

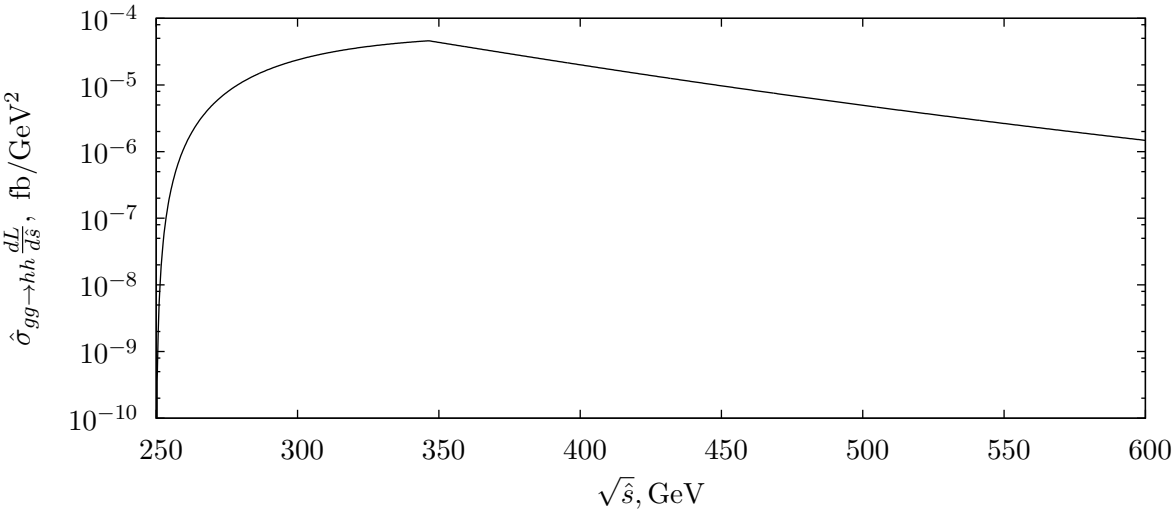

FIG. 7: Differential cross section for the $pp \to hh$ reaction at $\sqrt{s} = 14$ TeV.

Appendix B: Colored figures

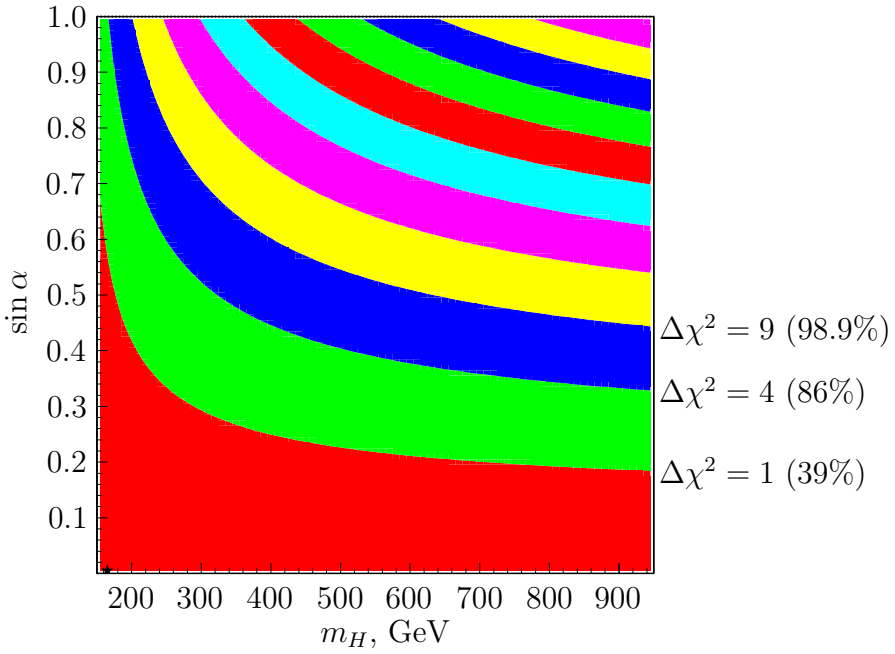

FIG. 2a: Bounds from electroweak precision observables.

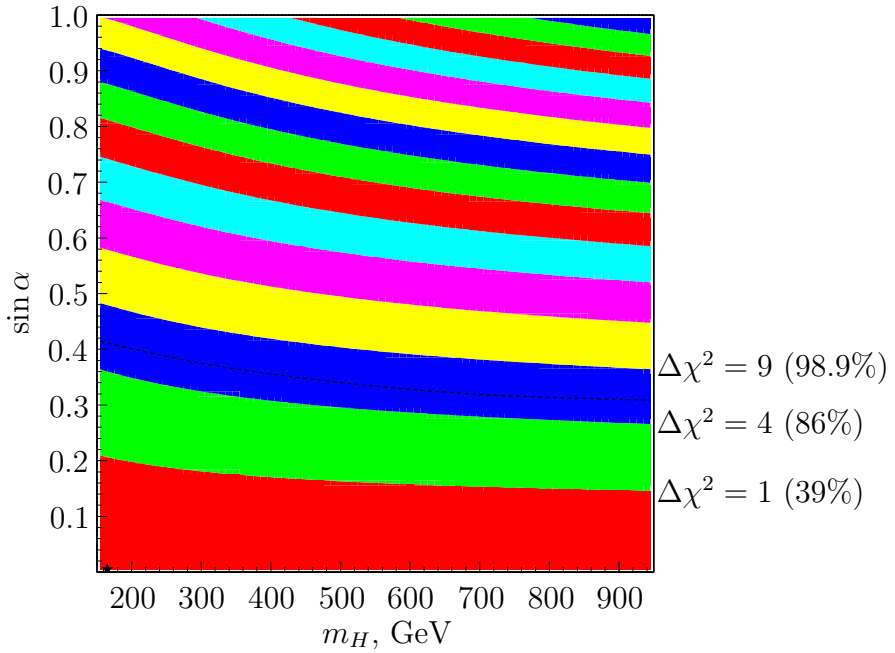

FIG. 2b: Bounds from both electroweak precision observables and signal strength measurements (11), (12). The dashed line corresponds to $\Delta\chi^2 = 5.99$; the probability that numerical values of $(m_H, \sin\alpha)$ are below it equals 95% (compare with Ref. [6], eq. (23)).

FIG. 2: Bounds on the singlet model parameters.

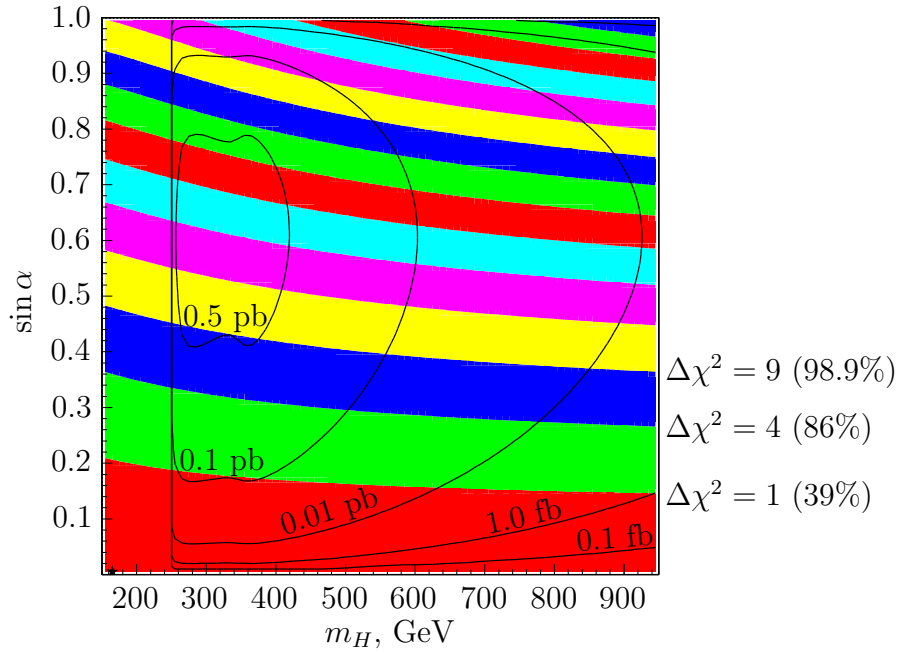

FIG. 4: Contour plot of $\sigma(pp \to H \to hh)$ for $\sqrt{s} = 14$ TeV. In this figure we neglect small effects of $H \to hh^*$.

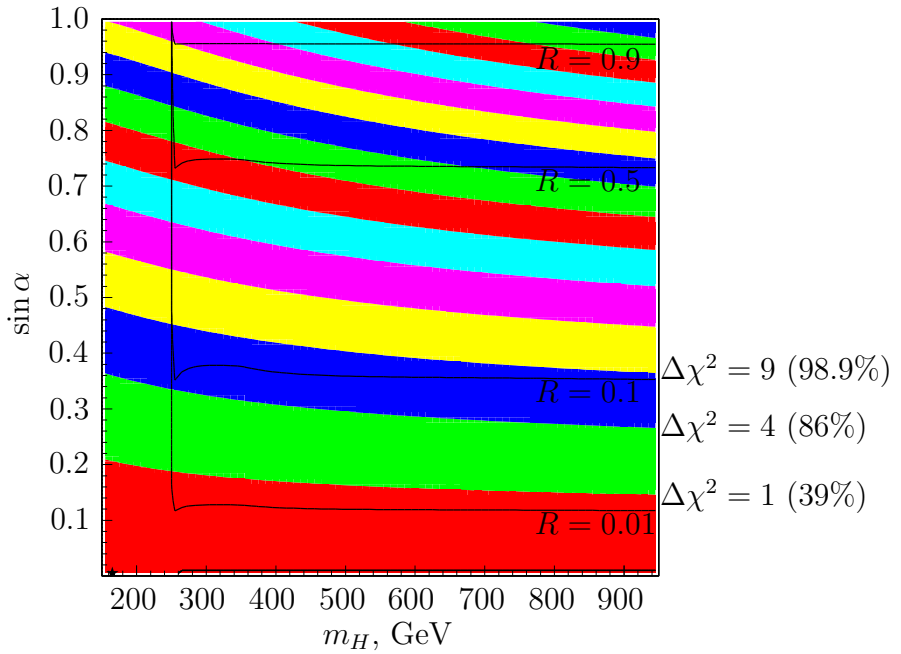

FIG. 5: Contour plot of $R \equiv \frac{\sigma(pp\to H)\mathrm{Br}(H\to ZZ)}{(\sigma(pp\to h)\mathrm{Br}(h\to ZZ))_{\mathrm{SM}}}$. In the calculation of R we assume $m_H > 2m_h$.

[1] The ATLAS collaboration, Phys. Lett. **B716** 1 (2012).

[2] The CMS collaboration, Phys. Lett. **B716** 30 (2012).

[3] Chien-Yi Chen, S. Dawson and I. M. Lewis, Phys. Rev. **D91** (2015) 035015, arXiv:1410.5488.

[4] T. Robens, T. Stefaniak, arXiv:1501.02234 (2015).

[5] V. Martin-Lozano, J. M. Moreno, C. B. Park, arXiv:1501.03799 (2015).

[6] A. Falkowski, C. Gross, O. Lebedev, arXiv:1502.01361 (2015).

[7] S. Godunov, M. Vysotsky, E. Zhemchugov, JETP Vol. 147 (3) (2015), arXiv:1408.0184.

[8] A. Hill, J. J. van der Bij, Phys. Rev. **D36**, 3463 (1987).

[9] The ATLAS collaboration, ATLAS-CONF-2014-009 (2014).

[10] The CMS collaboration, CERN-PH-EP-2014-288, CMS-HIG-14-009, arXiv:1412.8662, (2014).

[11] V. A. Novikov, L. B. Okun, A. N. Rozanov, M. I. Vysotsky, CPPM-95-1, arXiv:hep-ph/9503308.

[12] L. A. Harland-Lang, A. D. Martin, P. Motylinki, R. S. Thorne, arXiv:1412.3989 (2014).

[13] J. Baglio, A. Djouadi, JHEP 1103 (2011) 055, arXiv:1012.0530.

[14] L. B. Okun. *Leptons and Quarks.* World Scientific Publishing, Singapore, 2014. ISBN 978-981-4603-00-3.

[15] S. Dittmaier, C. Mariotti, G. Passarino et al., CERN-2011-002, arXiv:1101.0593.

[16] D. de Florian and J. Mazzitelli, PoS LL2014 (2014) 029, DESY 14-080 / LPN 14-073, arXiv:1405.4704.

[17] R. Contino et al., JHEP 1208 (2012) 154, arXiv:1205.5444.

[18] T. Plehn, M. Spira, and P. M. Zerwas. Nucl. Phys. B479, 46 (1996) [Erratum-ibid. B531, 655 (1996)], arXiv:hep-ph/9603205.

[19] X. Li, M. B. Voloshin. Phys. Rev. **D89** (2014) 1, 013012, arXiv:1311.5156.

[20] The CMS collaboration, CMS PAS HIG-13-002 (2013).

[21] S. Profumo, M. J. Ramsey-Musolf, G. Shaughnessy, JHEP 0708 (2007) 010, arXiv:0705.2425.
V. Barger, P. Langacker, M. McCaskey, M. J. Ramsey-Musolf, G. Shaughnessy, Phys. Rev. **D77** (2008) 035005, arXiv:0706.4311.
V. Barger, P. Langacker, M. McCaskey, M. J. Ramsey-Musolf, G. Shaughnessy, Phys. Rev. **D79** (2009) 015018, arXiv:0811.0393.

M. Gonderinger, Y. Li, H. Patel, M. J. Ramsey-Musolf, JHEP 1001 (2010) 053, arXiv:0910.3167.

M. Kadastik, K. Kannike, A. Racioppi, M. Raidal, JHEP 1205 (2012) 061, arXiv:1112.3647.

M. Gonderinger, H. Lim, M. J. Ramsey-Musolf, Phys. Rev. **D86** (2012) 043511, arXiv:1202.1316.

C. Caillol, B. Clerbaux, J. M. Frère, S. Mollet, Eur. Phys. J. Plus 129 (2014) 93, arXiv:1304.0386.

E. Gabrielli, M. Heikinheimo, K. Kannike et. al., Phys. Rev. **D89** (2014) 1, 015017, arXiv:1309.6632.

L. Basso, O. Fischer, J. J. van der Bij, Phys. Lett. B730 (2014) 326-331, arXiv:1309.8096.

J. M. No, M. J. Ramsey-Musolf, Phys. Rev. **D89** (2014) 9, 095031, arXiv:1310.6035.

J. de Blas, M. Chala, M. Pérez-Victoria, J. Santiago, CERN-PH-TH-2014-264, arXiv:1412.8480 (2014).

S. Profumo, M. J. Ramsey-Musolf, C. L. Wainwright, P. Winslow, Phys. Rev. **D91** (2015) 3, 035018, arXiv:1407.5342.

M. Gorbahn, J. M. No, V. Sanz, LTH 1039, arXiv:1502.07352 (2015).

D. Curtin, P. Meade, Ch-T. Yu, JHEP 1411 (2014) 127, arXiv:1409.0005.